

UDC 536.24

DOI: 10.31548/machinery/3.2023.79

Viktor Trokhaniak*

PhD in Technical Sciences, Associate Professor
National University of Life and Environmental Sciences of Ukraine
03041, 15 Heroiv Oborony Str., Kyiv, Ukraine
<https://orcid.org/0000-0002-8084-1568>

Valery Gorobets

Doctor of Technical Sciences, Professor
National University of Life and Environmental Sciences of Ukraine
03041, 15 Heroiv Oborony Str., Kyiv, Ukraine
<https://orcid.org/0000-0003-1180-4509>

Heat transfer and gas dynamics numerical modelling of compact pipe bundles of new design

Abstract. Weight and size characteristics, heat transfer efficiency across the surface, pressure losses in the flow paths for each heat transfer medium, and other parameters that characterise the heat exchanger play an important role in the development of new types of heat exchanger designs. This predefines the research relevance and the need for a solution. The research aims to develop and implement fundamentally new approaches to the design parameters of shell-and-tube heat exchangers, in which smooth-tube bundles are placed as compactly as possible in their crossflow. For this purpose, numerical modelling in the heat exchanger channels and studies of heat transfer and gas dynamics were carried out. The ANSYS Fluent software package was used to calculate the hydrodynamics and heat transfer in the tube bundle channels. Numerical modelling of hydrodynamics and heat transfer processes in the flow of a compact bundle of small-diameter pipes was carried out. The mathematical model includes the Navier-Stokes equation, the energy equation, and equations describing the turbulence of the external flow. The turbulence model $k-\varepsilon$ was chosen as a model that describes turbulence in channels well. The results of numerical modelling showed a compact bundle of pipes at the outlet of the channels, with an average value of $+20.1^{\circ}\text{C}$. Notably, the local temperature values near the channel walls are close to $+30^{\circ}\text{C}$. The air velocity at certain points of the duct reaches 85.1 m/s. At the same time, the average air velocity in the cross-section of the channel is about 41.2 m/s at $\text{Re} = 21420$. It is demonstrated that the maximum values of local heat transfer coefficients for pipes in a compact bundle are observed in the areas where the flow joins the pipe surface and at the beginning of the boundary layer formation. The maximum values of the heat transfer coefficient reach up to $1335.5 \text{ W/m}^2\text{C}$ for the second and third rows, and at the front point of the first order, it is $1042.3 \text{ W/m}^2\text{C}$. These results will improve the weight and dimensions of shell-and-tube heat exchangers and reduce their costs

Keywords: Navier-Stokes equation; Computational Fluid Dynamics; heat and mass transfer; intertubular channels; weight and dimensions

INTRODUCTION

A heat exchanger is a device used to efficiently transfer heat between two fluids (gas or liquid) to another. The use of heat exchangers in combination increases the efficiency of thermal management and energy saving of the system as

a whole (Hojjat, 2020). According to P. Bichkar *et al.* (2018), shell-and-tube heat exchangers have many applications in air conditioning, chemical engineering, power plants, and aerospace. They are divided into two categories based

Article's History: Received: 28.02.2023; Revised: 30.05.2023; Accepted: 11.08.2023.

Suggested Citation:

Trokhaniak, V., & Gorobets, V. (2023). Heat transfer and gas dynamics numerical modelling of compact pipe bundles of new design. *Machinery & Energetics*, 14(3), 79-89. doi: 10.31548/machinery/3.2023.79.

*Corresponding author



Copyright © The Author(s). This is an open access article distributed under the terms of the Creative Commons Attribution License 4.0 (<https://creativecommons.org/licenses/by/4.0/>)

on the direction of flow: straight tube and U-shaped. In straight-tube heat exchangers, the tube flow enters from one side of the heat exchanger and exits from the other side of the heat exchanger, but in U-tube heat exchangers, the flow enters the U-shaped tubes, returns, and exits from the same direction in which it enters.

Significant experimental and numerical research has been conducted on shell-and-tube heat exchangers to improve their efficiency (Wang *et al.*, 2020). In experimental studies, the cost of purchasing materials, parts, and the heat exchangers themselves is very high, so numerical modelling of heat exchangers using the commercial software package ANSYS. Fluent Theory Guide Release 18.2 (2017) is much more useful. This method considers all the details of geometry, and flow and can simulate the values of gas dynamics and heat transfer parameters at any point of the heat exchanger, but this method requires a lot of computer processing power.

M. Tayyab *et al.* (2020) claim that there are two ways to increase turbulence: active and passive. Active methods require the use of external energy, which can be mechanical, hydromagnetic or electrohydrodynamic (Alam & Kim, 2018). The use of extended surfaces called fins is a widely used passive method to increase heat transfer. M.T. Riaz *et al.* (2022) noted that the effective heat transfer area increases with the use of extended surfaces, which leads to flow turbulence, increasing the transfer rate. In the passive method, changing or improving the geometric properties of the flow path or adding intensifiers in the channel increases the intensity of turbulence in the fluid flow, resulting in an obvious increase in heat transfer rate. Passive methods of creating turbulence include twisted tubes, spiral strips, coils, and vortex flow generators (Feizabadi *et al.*, 2019; Talebi & Lalgani, 2021).

M.A. Jamil *et al.* (2020) used exergy-economic optimisation to improve the mass and thermal characteristics of heat exchangers. They achieved a reduction in heat exchange area by ~26.4%, capital cost by ~20%, operating cost by ~50%, total cost by ~22%, and flow cost by ~21%. T.-W. Lim & Y.-S. Choi (2020) developed the design and investigated the performance evaluation of a shell-and-tube heat exchanger utilising the cold energy of liquid natural gas on a ship washing the jacket of an internal combustion engine. The results of the cycle performance analysis show that R123 and R227e have the highest and lowest thermal efficiencies of approximately 17-23% and approximately 15-21%, respectively. R123 and R134a show the highest and lowest exergy efficiencies of approximately 25-31% and approximately 23-29%, respectively.

According to V. Gorobets *et al.* (2021), by varying the displacement of adjacent pipes in the transverse direction relative to the direction of flow in the channels, it is possible to improve the integrated characteristics of heat transfer on the surface of such bundles. Notably, these characteristics improve with an increase in the displacement of adjacent pipes, but at the same time, pressure losses in such channels increase. Therefore, when choosing the

geometry of a curved channel, one should limit the offset value, which, for example, for a pipe diameter of 10 mm in a bundle should not exceed 1-3 mm. V.I. Trokhaniak *et al.* (2023) found that for such bundles, the intensification of heat transfer does not require the use of high-power pumping equipment for pumping the heat carrier in the intertube channels of the heat exchanger.

Development and recommendation of both new and improved design solutions for shell-and-tube heat exchangers with a compact arrangement of tube bundles is a highly relevant research topic and requires a solution.

The research aims to improve the known and develop new designs of shell-and-tube heat exchangers with compact placement of smooth-tube bundles in their crossflow and to numerically simulate the processes of heat and mass transfer in the channels of these heat exchangers.

MATERIALS AND METHODS

All studies were carried out based on the problematic scientific laboratory “Heat and Mass Transfer Processes and Alternative Energy Sources” at the Department of Heat and Power Engineering of the National University of Life and Environmental Sciences of Ukraine. A shell-and-tube heat exchanger with a rectangular cross-section, in which tube bundles are arranged in a traditional staggered order with a step of $1.5 \times 1.5 (s_1/D \cdot s_2/D)$ and a compact configuration with their crossflow (Fig. 1) was considered. The heat exchanger uses a system of tubes in which adjacent tubes are in contact with each other and are displaced along the ordinate axes by a distance K relative to each other, where $0 < K < \sqrt{3}D/2$ distance meets the established condition $C \geq D + 5 \pm 0.1$ mm, where D is the outer diameter of the tubes. This is because modern and relatively cheap technologies for manufacturing such bundles are significantly complicated, with a distance between the tubes of less than 5 mm.

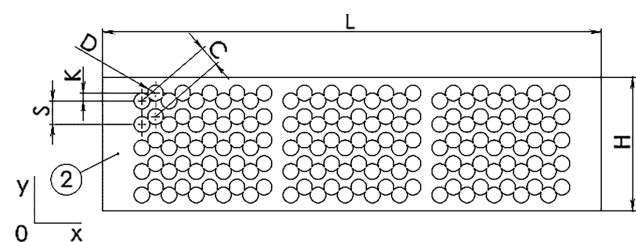


Figure 1.1. Tube board

with compact tube arrangement (top view)

Note: D – external tube diameter, m; S – width of the intertube passage, m; K – displacement of pipes along the ordinate axes, m; C – distance between pipes at displacement, m; L – length of the heat exchanger, m; H – heat exchanger width, m

Source: compiled by the authors

Numerical modelling of heat and mass transfer processes in the channels of heat exchangers of compact configuration was carried out using ANSYS software. Fluent theory guide. Release 18.2 (2017). The mathematical model is based on the Navier-Stokes equations (Khmelnik, 2010;

Marzouk *et al.* 2022) and the convective energy transfer equation. The standard $k-\varepsilon$ turbulence model was chosen (ANSYS..., 2017).

The Navier-Stokes equations describing heat and mass transfer in heat exchange channels in a two-dimensional system are as follows:

movement equation:

$$\rho \left(\frac{\partial u}{\partial t} + u \frac{\partial u}{\partial x} + v \frac{\partial u}{\partial y} \right) = -\frac{\partial p}{\partial x} + \mu \left(\frac{\partial^2 u}{\partial x^2} + \frac{\partial^2 u}{\partial y^2} \right), \quad (1)$$

$$\rho \left(\frac{\partial v}{\partial t} + u \frac{\partial v}{\partial x} + v \frac{\partial v}{\partial y} \right) = -\frac{\partial p}{\partial y} + \mu \left(\frac{\partial^2 v}{\partial x^2} + \frac{\partial^2 v}{\partial y^2} \right),$$

where ρ is the air density, kg/m³; μ is the dynamic air viscosity, Pa-s; p is the air pressure, Pa; u, v , is the vector field of air velocity, m/s; t is time, s;

equation of continuity:

$$\frac{\partial u}{\partial x} + \frac{\partial v}{\partial y} = 0; \quad (2)$$

energy conservation equation:

$$\rho C_p \left(V_x \frac{\partial T}{\partial x} + V_y \frac{\partial T}{\partial y} \right) = \frac{\partial}{\partial x} \left(\lambda \frac{\partial T}{\partial x} \right) + \frac{\partial}{\partial y} \left(\lambda \frac{\partial T}{\partial y} \right), \quad (3)$$

where T is the temperature at a certain point, °C; λ is the thermal conductivity of air, W/m·°K; C_p is the specific heat capacity of air, J/kg·°K.

Boundary conditions were set (Fig. 1) at inlet:

$$x=0; W=W_0; T=T_{inlet}, \quad (4)$$

at output:

$$x=H; \frac{\partial W}{\partial x} = 0, \quad (5)$$

tube walls:

$$T(x=x_{tube_int})(y=y_{tube_int}) = T_{wall_0}, \quad (6)$$

hull walls:

$$\left. \frac{\partial T_{wall_case}}{\partial y} \right|_{y=0} = 0, \quad (7)$$

adhesion conditions on the pipe wall:

$$x=x_{tube_int}; y=y_{tube_int}, \quad (8)$$

adhesion conditions on the hull wall:

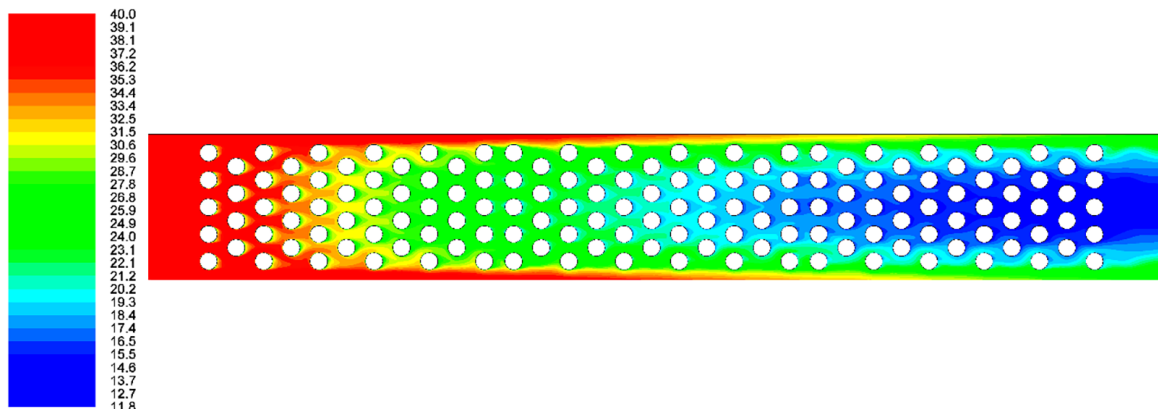


Figure 2. Temperature change in the heat exchanger staggered channel, °C

Source: V.I. Trokhaniak (2018)

$$y=H; W=0; y=0. \quad (9)$$

For the standard $k-\varepsilon$ turbulence model, the equations are as follows:

$$\frac{\partial}{\partial t}(\rho k) + \frac{\partial}{\partial x_i}(\rho k u_i) = \frac{\partial}{\partial x_j} \left[\left(\mu + \frac{\mu_t}{\sigma_k} \right) \frac{\partial k}{\partial x_j} \right] + G_k + G_b - \rho \varepsilon - Y_M + S_k \quad (10)$$

and

$$\frac{\partial}{\partial t}(\rho \varepsilon) + \frac{\partial}{\partial x_i}(\rho \varepsilon u_i) = \frac{\partial}{\partial x_j} \left[\left(\mu + \frac{\mu_t}{\sigma_\varepsilon} \right) \frac{\partial \varepsilon}{\partial x_j} \right] + C_{1\varepsilon} \frac{\varepsilon}{k} (G_k + C_{3\varepsilon} G_b) - C_{2\varepsilon} \rho \frac{\varepsilon^2}{k} + S_\varepsilon, \quad (11)$$

where G_k – generation of kinetic energy turbulence using velocity gradients; G_b – turbulence generation of kinetic energy from buoyancy; Y_M – dissipation contribution of the turbulence oscillating in the compressible to the total dissipation rate; $C_{1\varepsilon}$, $C_{2\varepsilon}$ and $C_{3\varepsilon}$ – constants; σ_k and σ_ε – turbulent Prandtl values for k and ε respectively.

The same boundary conditions apply in both cases. At the inlet of the heat exchanger, the mass flow rate is 0.25 kg/s at an initial temperature of $T_{inlet} = +40^\circ\text{C}$. The height of the pipes is 200 mm, their outer diameter is 10 mm, and their wall thickness is 1 mm. For the coolant flowing inside the pipes, the following boundary conditions were set, which are typical for the flow of liquid coolants in channels of this type: the temperature on the inner surface of the pipes of the first section, starting from the entrance to the pipe bundle, is $+11.46^\circ\text{C}$; for the second and third sections, respectively, $+10.88^\circ\text{C}$ and $+10.3^\circ\text{C}$. The width of this channel between the pipes in this bundle configuration is 5 mm.

RESULTS

Results of numerical modelling of a staggered and compact tube bundle of a new design

Figures 2 to 4 below show the results of a numerical simulation in the traditional staggered heat exchanger channels. As can be seen in Figure 2, the temperature of the heat transfer medium drops as it approaches the outlet of the heat exchanger. At the outlet, the average temperature across the channel width is $+19.3^\circ\text{C}$.

The velocity field in the heat exchanger and the duct shows that in certain parts of the duct, the air velocity near the walls reaches 41.2 m/s, and the average velocity in the narrowest section of the duct is about 31.1 m/s (Fig. 3).

Figure 4 shows the pressure field in the channels of the tested heat exchanger design. The obtained pressure distribution shows that the total pressure drop is about 3.8 kPa.

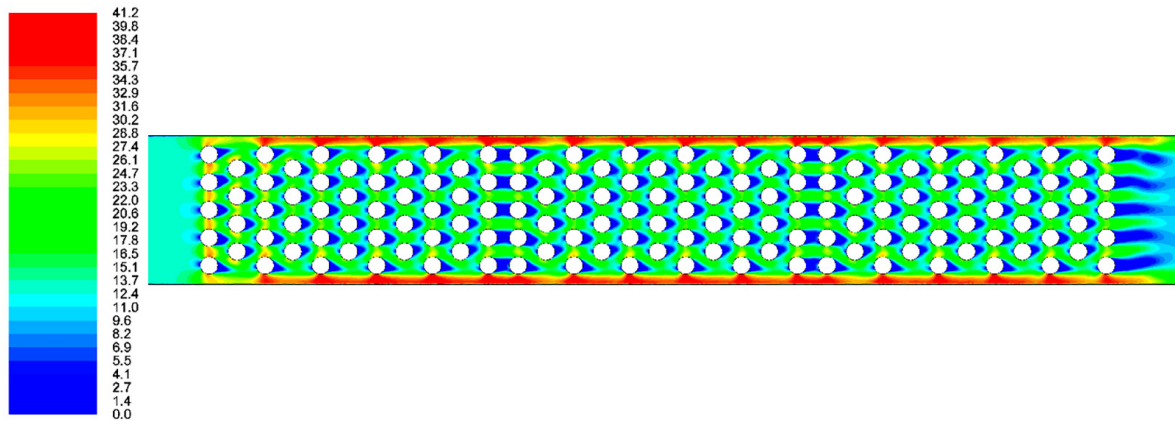


Figure 3. Velocity field in the staggered heat exchanger channel, m/s

Source: V.I. Trokhaniak (2018)

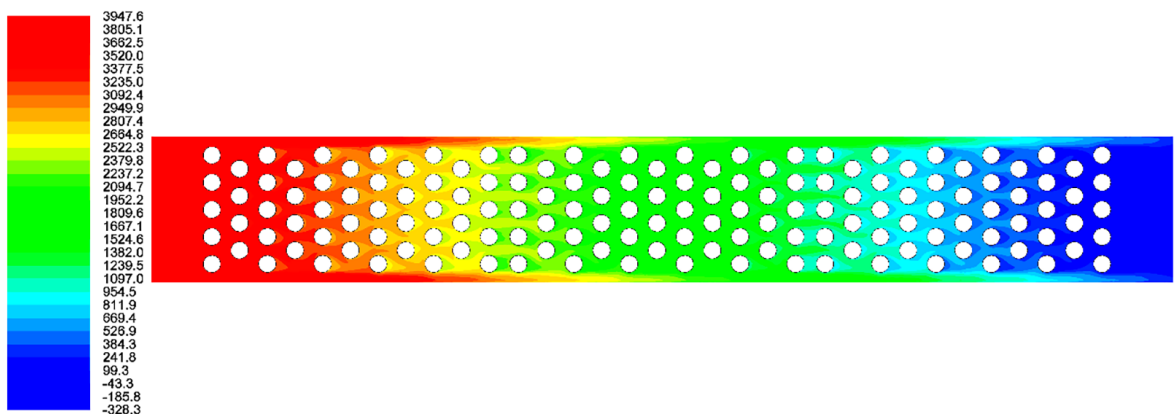


Figure 4. Pressure drop in the channel of the staggered beam, Pa

Source: V.I. Trokhaniak (2018)

As a result of the numerical modelling, the velocity field in the heat exchanger channels with a compact arrangement of the tube bundle was obtained, which is shown in Figure 5. Analysis of the results shows that the local velocity values reach their maximums and are observed in the areas adjacent to the side walls of the heat exchanger. It is characteristic that the local velocity values are twice as high as the average velocity values in the intertube channels. The analysis shows that at certain points in the channel, the air velocity can reach 85.1 m/s. At the same time, the average air velocity in the cross-section of the duct is about 41.2 m/s. Congestion zones are observed in certain sections of the duct in the pipe bundle. Congestion zones also occur in sections of the curved duct for areas located in the aft zone of the pipes.

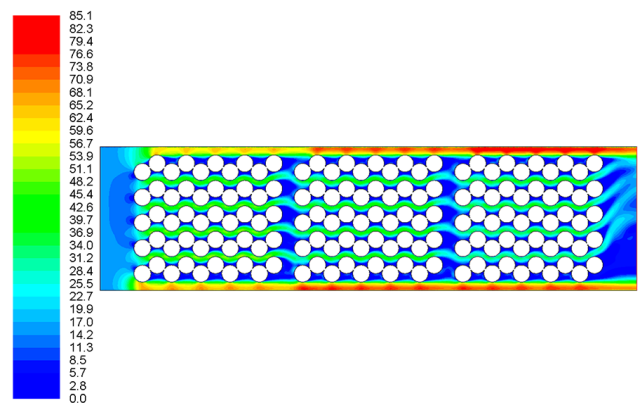


Figure 5. Air velocity in the compact beam channel, m/s
Source: compiled by the authors

Figure 6 the velocity vector distribution for a compact tube bundle. The lateral surface of an individual pipe is the first to be joined by the moulding flow and subsequently to detach the boundary layer. At the same time, congestion

zones are observed in the areas of the joints of neighbouring pipes. These zones are characterised by the presence of two separation vortices. The flow velocity in these zones is significantly lower than in the main flow.

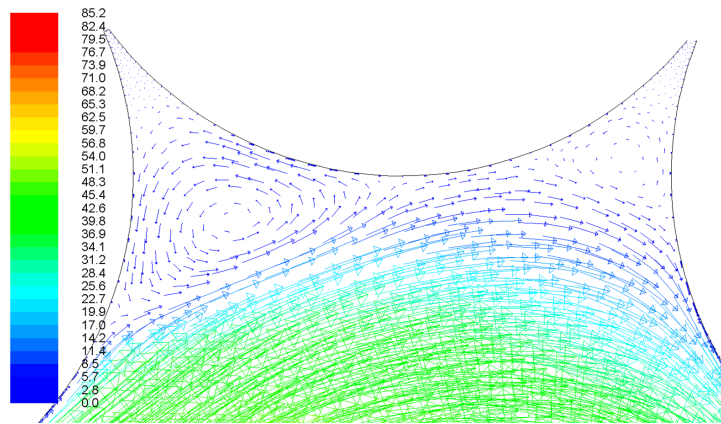


Figure 6. Velocity vector in the compact beam channel, m/s

Source: compiled by the authors

As a result of numerical modelling, the temperature field distributions in the channels of the tube bundle are shown in Figure 7. The analysis shows that the temperature of the heat carrier decreases as it approaches the outlet of the bundle channels. Assuming that the temperature at the inlet to the heat exchanger is +40°C, at the outlet of the channels its average value is +20.1°C. It is typical that near the channel walls, local temperature values are close to +30°C. Due to the high turbulence (at $Re = 21420$), the cold air flow at the outlet of the heat exchanger is slightly shifted upwards.

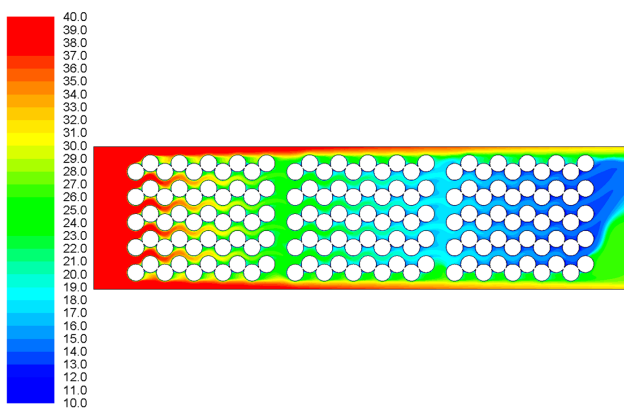


Figure 7. Temperature change in the compact beam channel, °C

Source: compiled by the authors

The pressure distributions in the channels of the compact tube bundle, acquired from numerical modelling, are shown in Figure 8.

The analysis of the found pressure fields shows that the pressure drop in this channel is about 7 kPa in total.

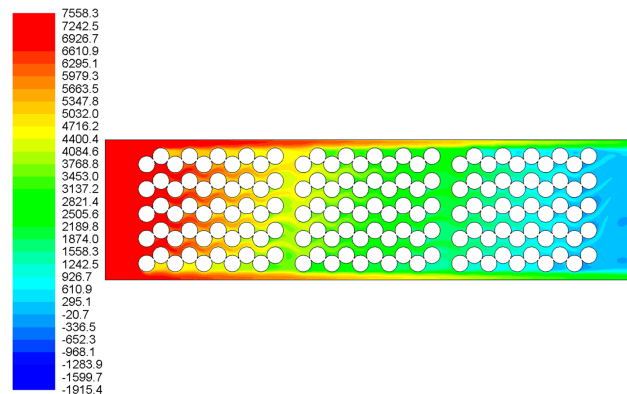


Figure 8. Pressure drop in the compact beam channel, Pa

Source: compiled by the authors

Local heat transfer results from a pipe bundle with a compact arrangement

Local distributions of the heat transfer coefficient around the circumference of the pipe reflect the main character of the influence of the heat exchange boundary layer on the pipe surface. By analysing the laws of this distribution, it is possible to determine the most ideal flow parameters, pipe arrangement in bundles and generalised relations for calculating the local heat transfer coefficient (Gorban *et al.*, 2021).

The specific heat transfer of a pipe in a bundle is the same as that of a local single pipe. The heat transfer distribution on the surface is determined by the flow properties of the pipe in the bundle, which are largely dependent on it. For a more detailed analysis of local heat transfer, Figure 9 shows the beginning and end of a pipe section. To improve the quality of the grid and obtain more detailed characteristics of the boundary layer, technical gaps were applied at the points of contact of neighbouring pipes (Fig. 9).

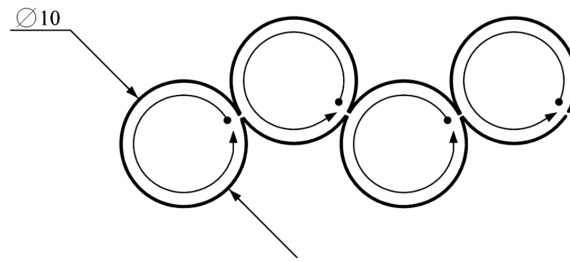


Figure 9. Start and end of the local heat distribution pipe section

Source: compiled by the authors

The peculiarities of the distribution of the local heat transfer coefficient in the first, second, and third rows were considered (Fig. 10).

Maximum values of the heat transfer coefficient, reaching up to $1335.5 \text{ W/m}^2\cdot^\circ\text{C}$ for the second and third rows, can be seen from the graph shown in Figure 10. As a result of the lateral influence of the flow, the process of flowing around the pipe of the second and all subsequent lines does not begin at the front point of the pipe, but at an angle of $\varphi = 151.1^\circ$. Subsequently, as the boundary lay-

er grows along the circumference of the pipe, heat transfer decreases. The heat transfer stabilises in the fourth row. The tubes of the second and subsequent rows are shaded by the first row in depth, so the heat transfer mode of the tubes in these rows differs from the heat transfer mode in the first row. At the front point, the first order is $1042.3 \text{ W/m}^2\cdot^\circ\text{C}$. The analysis of the change in local heat transfer in the tube bundle shows that the acceleration of the flow in its front part significantly affects the nature of the heat transfer distribution in all subsequent rows.

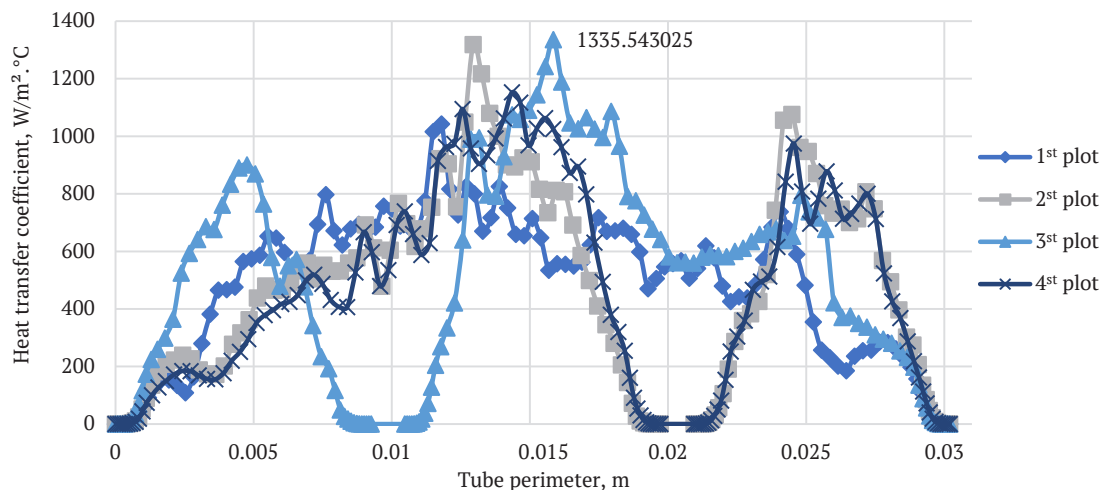


Figure 10. Local distribution of heat transfer from the pipe perimeter in a compact pipe bundle

Source: compiled by the authors

The uneven nature of the distribution of local values of heat transfer coefficients shown in Figure 10 is due to significant turbulence in the flow. Characteristically, for the first and third rows of pipes, there is a slight drop in heat transfer for an angle close to $\varphi \approx 290^\circ$, and then a slight increase in heat transfer occurs again due to an increase in the velocity gradient in the longitudinal direction. This is due to the presence of pipes that are located directly behind the individual pipe in the bundle. The heat flux density distribution plot for the first four rows located along the length of the channel is shown in Figure 11. The maximum value of

the local heat flux is about -29.44 kW/m^2 and is observed for the second and third rows. Figure 12 shows the local temperature distribution on the boundary layer, which reaches maximum values up to $291.1 \text{ }^\circ\text{K}$. The nature of the curves is somewhat similar to that of the heat transfer coefficient.

The weight and dimensions of a shell-and-tube heat exchanger with a staggered tube bundle arrangement (1.5×1.5) were compared with a heat exchanger of a new design, which uses a tube bundle with a compact arrangement of tubes. The results of comparing the characteristics obtained in the numerical modelling are presented in Table 1.

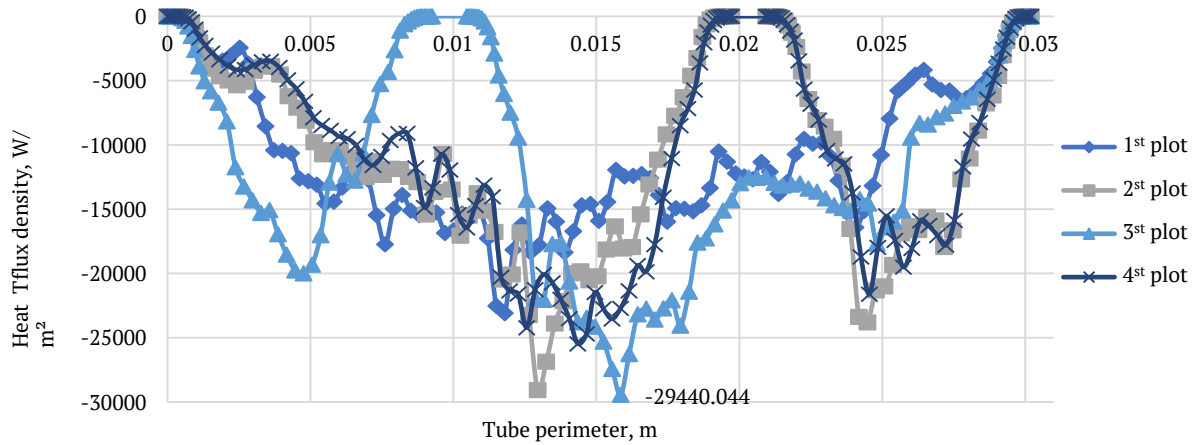


Figure 11. Local distribution of heat flux density from the pipe perimeter in a compact pipe bundle

Source: compiled by the authors

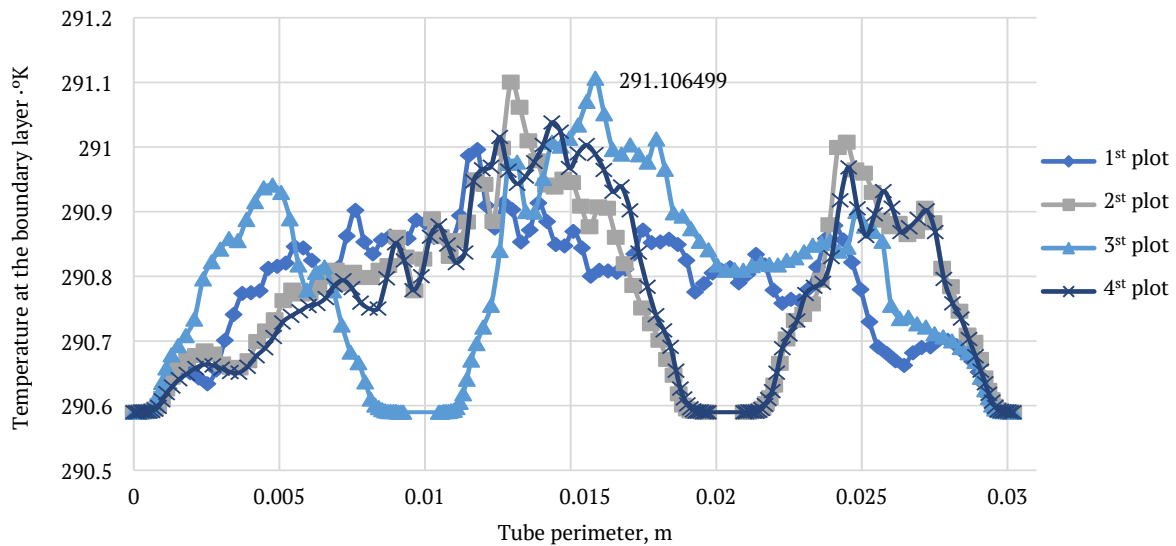


Figure 12. Local temperature distribution at the boundary layer from the pipe perimeter in a compact pipe bundle

Source: compiled by the authors

Table 1. Comparison of the weight and dimensions of a heat exchanger with a staggered (1.5x1.5) and compact tube bundle arrangement

The main parameter of the heat exchanger	Staggered tube bundle	Compact tube bundle
Heat output of the heat exchanger, W	5200	5000
Air temperature at the inlet to the heat exchanger, °C	+40	+40
Air temperature at the outlet of the heat exchanger, °C	+19.3	+20.1
Mass air flow rate, kg/s	0.25	0.25
Air heat transfer coefficient, W/m ² °C	314	321
Pressure drop at the inlet and outlet of the heat exchanger, Pa	3800	7560
Length of the heat exchanger, m	0.530	0.278
Pipe height in the bundle, m	0.20	0.20
Number of pipes, pcs.	150	150
Heat exchange mass, kg	16.6	15.2

Source: compiled by the authors

The data in Table 1 shows that with the same input parameters of the heat carrier and heat exchanger capacity, the difference between the values of heat transfer coefficients averaged over the pipe surface does not exceed 3%. A comparison of the geometric dimensions of the traditional and new heat exchangers shows that the latter reduces in size by 48% and in weight by 10%.

DISCUSSION

Heat exchangers are categorised either by flow configuration (counterflow, crossflow and crossflow) or by design (concentric tube, shell, and tube and compact) (Kundu *et al.* 2008). The ultimate goal of every heat exchanger or heat transfer study is to find methods or designs that increase the heat transfer rate. One of the main features of increasing heat transfer is changing the nature of the flow from laminar to turbulent (Rahman *et al.*, 2017). The greater the turbulence, the more it facilitates heat transfer (Alexandersson *et al.*, 2002; Zotloterer, 2004). In passive methods, the rate of heat transfer is increased by modifying the surfaces of the heat transfer interface (Lanjewar *et al.*, 2011; Hasanli *et al.*, 2022). For example, N. Nagarani *et al.* (2014) used the method of artificial roughness by using low height repeating ribs on the heat transfer surface to break the laminar layer and increase turbulence during heat transfer. M.A. Elyyan *et al.* (2008), and R. Bedi *et al.* (2018) described the use of V-shaped, W-shaped, angular, and transverse ribs to create artificial roughness. A. Erdogan & C. Ozgur Colpan (2018) based the development of the problem on a shell-and-tube heat exchanger that combines a parabolic trough solar collector and an organic Rankine cycle. This allowed the total heat transfer coefficient to be reduced from 1579 to 1491 W/m²K, the heat transfer surface area to be increased from 7 to 25.25 m², and the pumping power to be increased from 0.8723 to 0.9227 kW.

A twisted tube heat exchanger is a heat exchanger that increases the heat transfer coefficient on the tube side (Gu *et al.*, 2020). X.Z. Li *et al.* (2019) conducted a numerical study of the crossflow of twisted oval tube bundles with a linear arrangement and presented empirical correlations for the Nusselt number and Euler number. In addition, it was found that the velocity and temperature fields are periodically repeated every $S/2$ along the twisted oval tube. Z. Yang *et al.* (2020), N. Biçer *et al.* (2021), and A.C. Caputo *et al.* (2022) considered shell-and-tube heat exchangers with a modified design, which differ significantly from the traditional type.

It should be noted that the analysis of the numerical modelling of heat exchangers with a traditional staggered and compact arrangement of tubes in a bundle makes it possible to improve the weight and dimensions of shell-and-tube heat exchangers. The main difference between the new design of the heat exchanger and the traditional one is that it uses rows of small diameter tubes that are arranged without a gap between the tubes in the flow direction (Kundu *et al.* 2008; Lanjewar *et al.*, 2011). In addition, the neighbouring pipes are offset by a certain distance,

which can vary from minimal values to a value of half the pipe diameter. This makes it possible to reduce the longitudinal dimensions of the heat exchanger by 1.5-2 times while reducing the mass of the heat exchanger by 10-15% compared to the work of M.A. Jamil *et al.* (2020). The use of continuous rows of pipes with an offset creates channels of a curved configuration in the heat exchanger, which leads to the intensification of heat transfer in the channels with a moderate increase in hydraulic losses when pumping the coolant (air) in the intertube channels.

Another important aspect of numerical modelling is the analysis of local distributions of temperatures, velocities, and pressures in curved channels. The local distributions of heat transfer coefficients, heat flux density and temperatures on the pipe surface indicate the surface areas where the local values of these parameters will be maximum. Such local extremes occur at the points where the connected flow enters after the breakaway zones formed in the recesses of curved channels, where the coolant velocity is significantly lower than in the main flow. At the points of connection of the external flow to the pipe surface, the beginning of the boundary flow is formed, where its thickness will be minimal, and the heat transfer coefficients and density of the diverted heat flow will be maximum.

The next conclusion that can be drawn from the analysis of the numerical calculation results is as follows. As follows from the local velocity distributions in the channels of the new design heat exchanger, the flow velocity near the side walls of the shell is 1.5-2 times higher than the coolant velocity in the curved channels. This leads to a redistribution of the coolant flow rate near the shell walls, which is not accompanied by an intensification of heat transfer for the extreme pipe bundles (Yang *et al.*, 2020; Biçer *et al.*, 2021; Caputo *et al.*, 2022). Therefore, to improve heat transfer for the entire bundle, it is necessary to minimise the width of the channels near the shell walls, which is due to the production technology of shell-and-tube heat exchangers, namely, the minimum distance between the pipes and the shell body when welding the pipes to the tube board and the heat exchanger shell.

The limiting case of the considered heat exchanger design with a compact pipe arrangement is the case when the displacement between adjacent pipes is zero. In this case, the hydraulic losses for pumping the coolant (air) will be minimal, and the average value of the heat transfer coefficient over the pipe surface will decrease. To increase it, it is necessary to increase the flow rate of the coolant or the average velocity of the coolant in the inter-pipe channels. Such a design of the tube bundles of a shell-and-tube heat exchanger is advisable to use, for example, for heat recovery units in cogeneration plants, where pressure losses are limited by the limit values of the pressure at the exhaust of exhaust products of internal combustion engines.

Thus, it can be generally concluded that the proposed new design of the shell-and-tube heat exchanger has advantages over known designs and can be used in the design of heat exchangers for various purposes.

CONCLUSIONS

New design solutions for a compact tube bundle of a shell-and-tube heat exchanger used for heating and cooling the supply air in poultry house ventilation systems for the summer and winter seasons have been proposed. Numerical modelling of gas dynamics and heat transfer processes in the channels of the proposed and staggered (1.5×1.5) tube bundle and in heat exchangers was carried out using ANSYS Fluent software. As a result, the temperature fields, velocities, and pressures in the studied channels of the tube bundles were obtained for staggered and compact arrangements. The obtained distributions are analysed and the ways to improve the heat transfer conditions in the channels with a compact arrangement of pipes are indicated. A method of calculation on the surface of the pipe bundle is proposed for determining the average values of the heat transfer coefficient.

As a result of the analysis of the obtained distribution of local heat transfer, a maximum value of about 1335.5 W/m²·°C is observed on the first four rows, and the heat flux density is 29.44 kW/m² at an angle of $\varphi = 151.1^\circ$. At the frontal point of the first row, the heat transfer coefficient is 1042.3 W/m²·°C. Between the tubes, when they touch each other, local heat transfer is significantly reduced due to a drop in velocity and the creation of stagnant airflow zones. To increase the local heat transfer distributions and increase the efficiency of the heat exchanger, it is

necessary to reduce the stagnant zones between the tubes in the future. Based on the analysis of numerical modelling, it can also be suggested to further reduce the distance between the outermost tubes and the heat exchanger shell (body). These actions will reduce the amount of air in these areas, and in turn, the airflow and Re number will increase in the channels between the tubes. This will be accompanied by an increase in both local and average heat transfer in compact tube bundles.

The weight and size characteristics of traditional designs of a shell-and-tube heat exchanger and a heat exchanger using a new compact bundle of small-diameter pipes with the same heat output were compared. The advantages of the new design of the heat exchanger are shown, which consist of reducing the overall dimensions by 48% and reducing the weight by 10%. In the future, to increase heat transfer, the authors recommend investigating compact tube bundles with the addition of heat transfer intensifiers in the form of fins.

ACKNOWLEDGEMENTS

To the Ministry of Education and Science of Ukraine for financial support of projects of young scientists (Kyiv), No. 110/1M-pr-2022.

CONFLICT OF INTEREST

The authors declare no conflict of interest.

REFERENCES

- [1] Alam, T., & Kim, M.H. (2018). A comprehensive review on single phase heat transfer enhancement techniques in heat exchanger applications. *Renewable and Sustainable Energy Reviews*, 81, 813-839. doi: 10.1016/j.rser.2017.08.060.
- [2] Alexandersson, O., Zweigbergk, K., & Zweigbergk, C. (2002). *Living Water: Viktor Schauberg and the secrets of natural energy*. Dublin: Gill Books Gateway.
- [3] ANSYS. Fluent theory guide. Release 18.2. (2017). Retrieved from https://www.luis.uni-hannover.de/fileadmin/software-lizenzen/Ueberlassung/ANSYS18.2_ReleaseNotes.pdf.
- [4] Bedi, R., Kiran, K., Mulla, A.M., Manoj, & Hebbar, G.S. (2018). Experimental augmentation of heat transfer in a shell and tube heat exchanger using twisted tape with baffles and hitrain wire matrix inserts – a comparative study. *IOP Conference Series: Materials Science and Engineering*, 376, article number 012003. doi: 10.1088/1757-899X/376/1/012003.
- [5] Biçer, N., Engin, T., Yaşar, H., Büyükkaya, E., Aydın, A., & Topuz, A. (2021). Design optimization of a shell-and-tube heat exchanger with novel three-zonal baffle by using CFD and taguchi method. *International Journal of Thermal Sciences*, 155, article number 106417. doi: 10.1016/j.ijthermalsci.2020.106417.
- [6] Bichkar, P., Dandgaval, O., Dalvi, P., Godase, R., & Dey, T. (2018). Study of shell and tube heat exchanger with the effect of types of baffles. *Procedia Manufacturing*, 20, 195-200. doi: 10.1016/j.promfg.2018.02.028.
- [7] Caputo, A.C., Federici, A., Pelagagge, P.M., & Salini, P. (2022). On the selection of design methodology for shell-and-tube heat exchangers optimization problems. *Thermal Science and Engineering Progress*, 34, article number 101384. doi: 10.1016/j.applthermaleng.2022.118541.
- [8] Elyyan, M.A., Rozati, A., & Tafti, D.K. (2008). Investigation of dimpled fins for heat transfer enhancement in compact heat exchangers. *International Journal of Heat and Mass Transfer*, 51, 2950-2966. doi: 10.1016/j.ijheatmasstransfer.2007.09.013.
- [9] Erdogan, A., & Ozgur Colpan, C. (2018). Thermal design and modeling of shell and tube heat exchangers combining PTSC and ORC systems. *Exergetic, Energetic and Environmental Dimensions*, 2018, 279-305. doi: 10.1016/B978-0-12-813734-5.00016-0.
- [10] Feizabadi, A., Khoshvaght-Aliabadi, M., & Rahimi, A.B. (2019). Experimental evaluation of thermal performance and entropy generation inside a twisted U-tube equipped with twisted-tape inserts. *International Journal of Thermal Sciences*, 145, article number 106051. doi: 10.1016/j.ijthermalsci.2019.106051.

- [11] Gorban, V.F., Andreev, A.O., Stolbovy, V.O., Firstov, S.O., & Karpets, M.V. (2021). [Influence of the lattice parameter on physical properties of high-entropy coatings](#). *Scientific Herald of Uzhhorod University. Series "Physics"*, 49, 61-65.
- [12] Gorobets, V., Trokhaniak, V., Bohdan, Y., & Antypov, I. (2021). Numerical modeling of heat transfer and hydrodynamics in compact shifted arrangement small diameter tube bundles. *Journal of Applied and Computational Mechanics*, 7(1), 292-301. [doi: 10.22055/JACM.2020.31007.1855](#).
- [13] Gu, H., Chen, Y., Sund'en, B., Wu, J., Song, N., & Su, J. (2020). Influence of alternating V- rows tube layout on thermal-hydraulic characteristics of twisted elliptical tube heat exchangers. *International Journal of Heat and Mass Transfer*, 159, article number 120070. [doi: 10.1016/j.ijheatmasstransfer.2020.120070](#).
- [14] Hasanli, R., Aliyev, I., Poladov, N., Azimova, L., & Tagiyev, T. (2022). Isothermal transformations in high-strength cast iron. *Scientific Herald of Uzhhorod University. Series "Physics"*, 51, 48-58. [doi: 10.54919/2415-8038.2022.51.48-58](#).
- [15] Hojjat, M. (2020). Nanofluids as coolant in a shell and tube heat exchanger: ANN modeling and multi-objective optimization. *Applied Mathematics and Computation*, 365, article number 124710. [doi: 10.1016/j.amc.2019.124710](#).
- [16] Jamil, M.A., Goraya, T.S., Shahzad, M.W., & Zubair, S.M. (2020). Exergoeconomic optimization of a shell-and-tube heat exchanger. *Energy Conversion and Management*, 226, article number 113462. [doi: 10.1016/j.enconman.2020.113462](#).
- [17] Khmelnik, S.I. (2010). [Navier-Stokes equations. On the existence and the search method for global solutions](#). Charleston: CreateSpace Independent Publishing Platform.
- [18] Kundu, P.K., Cohen, I.M., & Dowling, D.R. (2008). [Fluid mechanics](#) (4 Ed.). Amsterdam: Elsevier.
- [19] Lanjewar, A., Bhagoria, J.L., & Sarviya, R.M. (2011). Heat transfer and friction in solar air heater duct with W-shaped rib roughness on absorber plate. *Energy*, 36, 4531-4541. [doi: 10.1016/j.energy.2011.03.054](#).
- [20] Li, X.Z., Zhu, D.S., Yin, Y.D., Tu, A., & Liu, S.J. (2019). Parametric study on heat transfer and pressure drop of twisted oval tube bundle with in line layout. *International Journal of Heat and Mass Transfer*, 135, 860-872. [doi: 10.1016/j.ijheatmasstransfer.2019.02.031](#).
- [21] Lim, T.-W., & Choi, Y.-S. (2020). Thermal design and performance evaluation of a shell-and-tube heat exchanger using LNG cold energy in LNG fuelled ship. *Applied Thermal Engineering*, 171, article number 115120. [doi: 10.1016/j.applthermaleng.2020.115120](#).
- [22] Marzouk, S.A., Abou Al-Sood, M.M., El-Fakharany, M.K., & El-Said, E.M.S. (2022). A comparative numerical study of shell and multi-tube heat exchanger performance with different baffles configurations. *International Journal of Thermal Sciences*, 179, article number 107655. [doi: 10.1016/j.ijthermalsci.2022.107655](#).
- [23] Nagarani, N., Mayilsamy, K., Murugesan, A., & Kumar, G.S. (2014). Review of utilization of extended surfaces in heat transfer problems. *Renewable and Sustainable Energy Reviews*, 29, article number 604613. [doi: 10.1016/j.rser.2013.08.068](#).
- [24] Rahman, M.M., Tan, J.H., Fadzilita, M.T., & Muzammil, A.W.K. (2017). A review on the development of gravitational water vortex power plant as alternative renewable energy resources. *IOP Conference Series: Materials Science and Engineering*, 217, article number 012007. [doi: 10.1088/1757-899X/217/1/012007](#).
- [25] Riaz, M.T., Cheema, T.A., Tayyab, M., Khan, A.U.A., Amber, K.P., Sajid, M.B., Park, C.W. (2022). Investigation of free and forced vortex induced thermal energy exchange potential. *Sustainable Energy Technologies and Assessments*, 52, article number 102107. [doi: 10.1016/j.seta.2022.102107](#).
- [26] Talebi, M., & Lalgani, F. (2021). Assessment of thermal behavior of variable step twist in the elliptical spiral. *International Journal of Thermal Sciences*, 170, article number 107126. [doi: 10.1016/j.ijthermalsci.2021.107126](#).
- [27] Tayyab, M., Cheema, T.A., Malik, M.S., Muzaffar, A., Sajid, M.B., & Park, C.W. (2020). Investigation of thermal energy exchange potential of a gravitational water vortex. *Renewable Energy*, 162, 1380-1398. [doi: 10.1016/j.renene.2020.08.097](#).
- [28] Trokhaniak, V., Gorobets, V., Shelimanova, O., & Balitsky, A. (2023). Research of thermal and hydrodynamic flows of heat exchangers for different air cooling systems in poultry houses. *Machinery & Energetics*, 14(1), 68-78. [doi: 10.31548/machinery/1.2023.68](#).
- [29] Trokhaniak, V.I. (2018). *Power saving system in poultry-houses with usage of soil low-potential energy*. Kyiv: Komprint.
- [30] Wang, C., Cui, Z., Yu, H., Chen, K., & Wang, J. (2020). Intelligent optimization design of shell and helically coiled tube heat exchanger based on genetic algorithm. *International Journal of Heat and Mass Transfer*, 159, article number 120140. [doi: 10.1016/j.ijheatmasstransfer.2020.120140](#).
- [31] Yang, Z., Ma, Y., Zhang, N., & Smith, R. (2020). Design optimization of shell and tube heat exchangers sizing with heat transfer enhancement. *Computers & Chemical Engineering*, 137, article number 106821. [doi: 10.1016/j.compchemeng.2020.106821](#).
- [32] Zotloterer, F. (2004). Hydroelectric power station. Austria Patent AU2003294512. Retrieved from <https://patents.google.com/patent/AU2003294512A1/en>.

Віктор Іванович Троханяк

Кандидат технічних наук, доцент
Національний університет біоресурсів і природокористування України
03041, вул. Героїв Оборони, 15, м. Київ, Україна
<https://orcid.org/0000-0002-8084-1568>

Валерій Григорович Горобець

Доктор технічних наук, професор
Національний університет біоресурсів і природокористування України
03041, вул. Героїв Оборони, 15, м. Київ, Україна
<https://orcid.org/0000-0003-1180-4509>

**Чисельне моделювання теплообміну та газодинаміки
компактних пучків труб нової конструкції**

Анотація. При розробці нових типів конструкцій теплообмінних апаратів важливу роль відіграють такі фактори, як їх масогабаритні характеристики, ефективність теплопереносу через поверхню, що розділяє теплоносії, втрати тиску в трактах для кожного з теплоносіїв та інші параметри, які характеризують теплообмінний апарат. Таким чином, наукові дослідження у даній сфері є актуальними і вимагають свого рішення. Мета роботи полягала у розробці та впровадженні принципово нових підходів конструкційних параметрів кожухотрубних теплообмінників, у яких гладкотрубні пучки розміщені якомога компактно при їх поперечному обтіканні. Для цього було проведено чисельного моделювання в каналах теплообмінників і дослідження процесів теплообміну та газодинаміки. Для розрахунку гідродинаміки і теплопереносу в каналах трубного пучка використовували пакет прикладних програм ANSYS Fluent. Проведено чисельне моделювання процесів гідродинаміки і теплопереносу при обтіканні компактного пучка труб малого діаметра. Математична модель включає рівняння Нав'є-Стокса, рівняння енергії і рівняння, які описують турбулентність зовнішнього потоку. В якості моделі турбулентності вибрана $k-\varepsilon$ модель, яка добре описує турбулентність в каналах. Результати чисельного моделювання показали на виході з каналів компактного пучка труб, усереднене значення якого складає $+20,1^{\circ}\text{C}$. Характерно, що поблизу стінок каналу локальні значення температур мають значення близькі до $+30^{\circ}\text{C}$. Швидкість повітря в окремих точках каналу досягає $85,1$ м/с. При цьому середня швидкість повітря в поперечному перерізі каналу має значення близько $41,2$ м/с при $\text{Re} = 21420$. Продемонстровано, що максимальні значення локальних коефіцієнтів тепловіддачі для труб в компактному пучку спостерігаються в областях приєднання потоку до поверхні труб і на початку формування межового шару. Максимальні значення коефіцієнта тепловіддачі, що досягає до $1335,5$ Вт/м²°C для другого та третього рядів, а у передній точці першого порядку становить $1042,3$ Вт/м²°C. Отримані результати дадуть змогу покращити масогабаритні показники кожухотрубних теплообмінників та знизити їх собівартість

Ключові слова: рівняння Нав'є-Стокса; Computational Fluid Dynamics; тепломасообмін; міжтрубні канали; масогабаритні показники